13th International Conference on
Structural Health Monitoring of Intelligent Infrastructure
DOI: 10.3217/978-3-99161-057-1-160

Efficacy of decoupling techniques to extract the static strain response from the dynamic response of a bridge under a moving vehicle using a low pass filter

Sarath R.[1,0000-0001-6208-253X], Saravanan U.[1, 0000-0001-8565-0632]
[1]Department of Civil Engineering, Indian Institute of Technology Madras, Chennai 600 036, Tamil Nadu, India
email: sarathramesh09@gmail.com, saran@iitm.ac.in

ABSTRACT: Structural Health Monitoring of bridges is being used increasingly to ensure safe operation of bridges. Non-iterative and mechanics-based algorithms that were developed in the past to find the material property of a bridge or the live load moving over the bridge use the static strain response of the bridge. However, the field strain measurement of these response quantities has both static and dynamic components. To apply these non-iterative methods for live load or material property estimation, it is important to decouple the static components of the strain from its dynamic components. Hence, in the current study, the dynamic components of the bridge strain response are filtered to extract the static components using a low-pass filter. The adequacy of filtering is then measured based on the probability of the static maximum axial strain and average shear strain contained in the probabilistically determined dynamic response corresponding to different road roughness. The idea of relating the cutoff frequency to the bridge natural frequency is investigated. It is concluded that using a cutoff frequency of half the bridge natural frequency, one can sufficiently filter out the dynamic components under any case of vehicle speed, road roughness, and bridge natural frequency.

KEY WORDS: System identification; Dynamic response filtering; Monte Carlo simulation; Vehicle bridge interaction; Low-pass filter.

1 INTRODUCTION

Bridges play a critical role in a country's development. The bridges built in the past are deteriorating due to degradation from the environment and varying operational conditions. Although the current method of visual inspection is simple in procedure, it has some disadvantages when dealing with many bridges. It is time-consuming and subjective. Hence, structural health monitoring (SHM) is emerging as a viable alternative. SHM uses technology to access the current state of the bridge. The current state of the bridge here refers to either the current stiffness or the strength of the bridge. The strength is determined by non-destructive testing, like the rebound hammer and ultrasonic pulse velocity. In contrast, stiffness is determined by knowing the material parameters, boundary conditions, geometric parameters, and live load spectrum.

In the present study, the focus is on determining the current stiffness of the bridge. This can be computed by finding the current material properties and geometrical quantities like the moment of inertia and the cross-sectional area. To do so, the usual approach is to minimize the error between the measured response and the computed response using an optimization algorithm. But this involves computational costs, the problem being ill-posed, and other disadvantages. So, a mechanics-based non-iterative algorithm was proposed [1] to estimate the material property. This method has been proven effective for quasi-static loading conditions, neglecting vehicle-bridge interaction (VBI) dynamics. However, when it comes to realistic traffic scenarios and road roughness profiles, VBI is present and leads to a deviation of the measured response from the actual static response. So, one needs to filter out the dynamic components to arrive closer to the static response.

Now, the input to the material parameter estimation algorithm can be given in two ways. Either a known vehicle load will move over the bridge, as in [1] or the vehicle load also needs to be found using some appropriate measured response quantity [2]. The latter is more advantageous than the former in the case of continuous monitoring. So, identifying the moving load is also focused on. In general, moving load identification literature again involves optimization-based algorithms with the above-mentioned disadvantages. The numerous vehicles and bridge parameters must be known or optimized to find the axle loads. Such an approach increases the uncertainty involved in fixing the parameter values or ill-posed problem and hence reduces the accuracy of the identification. Instead, an algorithm for load estimation in a railway bridge was proposed by [2], which uses a composite strain response for estimating the moving load. An important property of this composite response is that it remains constant over a period for a single vehicle to pass over the bridge. But once again, the field-measured value of this composite strain response quantity can potentially include the dynamic components due to VBI and does not remain constant.

To overcome the above-mentioned difficulties, one of the approaches followed is to filter out the dynamic components from the measured response to get the static response. Few works on filtering can be found in the literature. For instance, in [3], a digital filtering technique was employed to obtain the static bridge response from the dynamic weigh-in-motion data. A low-pass filter of frequency ranging from 0.25 Hz to 1.0 Hz was used. But later it was shown that no proper criteria can be found for cutoff frequency, and a new technique called the equivalent digital filtering technique (EDFT) was proposed [4]. This uses the pseudo-static response of the bridge and the fact

DOI: 10.3217/978-3-99161-057-1-160

that the dynamic response (pseudo-static response + dynamic effects) and the static response in the frequency domain are approximately equal at 0 Hz. It was shown to be highly accurate in estimating static vehicle weight on dynamic response untainted by other miscellaneous vibrations. [5] used an 11-point and 21-point moving average low-pass filter to improve the accuracy of identified moving loads by eliminating the noise effect. It was found that the percentage errors were significantly reduced, and hence filtering was highly recommended. [6] used a low-pass filter to filter out the dynamic components from the identified bridge influence lines. In [7], the noise and dynamic components are removed to get static strains for moving load identification. It was found that when the cutoff frequency is equal to six to eight times the fundamental frequency of the train load, the peaks of the second derivative of the strain measurements can be identified. Recently, [8] used a low-pass filter to isolate the bridge response from the vehicle dynamics and other excitation sources (the asphalt roughness). The acceleration signal from a vehicle moving at 140 km/h was filtered to obtain the static response for identification of the bridge's elastic modulus using the correlation method. A cutoff frequency of 0.5 Hz, much less than the vehicle's first natural frequency of 2 Hz, was used. It was shown that proper filtering could adequately filter out the vehicle dynamics and other excitations. Now, even though many studies on filtering are available, there are not many studies that extensively deal with measuring the efficacy of filtering algorithms for various vehicle bridge parameters.

Hence, in the present study, a methodology to filter out the dynamic components from the measured strain response is developed. A numerical simulation is performed by modeling the vehicle bridge interaction dynamics. Using a half-car model and a classical Euler-Bernoulli beam model, the dynamic characteristics of the bridge strain response are obtained. Then, using a low-pass filter based on a cutoff frequency, the high frequency components are filtered out. The degree of closeness of the static response is measured using a probabilistic measure. The working of the proposed method is checked for the practical range of vehicle and bridge parameters.

In this paper, the methodology adopted in the study is explained in Section 2, followed by the implementation details of VBI modelling, code validation, numerical data taken in the study, and modal convergence in Section 3. The investigation relating the cutoff frequency to the bridge natural frequency and the effect of various VBI parameters is illustrated in Section 4. Finally, the study is summarized, and the findings from the study are listed in Section 5.

2 METHODOLOGY

The Fast Fourier Transform (FFT) of the bridge response was computed to understand its various frequency components. The FFT of the mid-span bridge acceleration response and the bridge mid-span axial strain response is shown in Figure 1. It is observed that the dynamic components are predominant in the acceleration FFT, whereas the static components are predominant in the strain FFT. Hence, it can be observed that when one uses strain response, the feasibility of getting the static response is much higher than that of using the acceleration response. So, through a threshold frequency called "cutoff frequency", one can segregate the static and dynamic components. First, the dynamic analysis is performed using a half-car vehicle model. The dynamic responses of concern in the study are the maximum mid-span axial strain and the mean of the sum of shear forces at the quarter span and the three-quarter span. The reason for choosing them is because of their applicability in non-mechanics-based SHM algorithms. The maximum mid-span axial strain is used in finding the material property of the bridge [1] and the average shear strain is used in estimating the moving load [2]. A Monte Carlo simulation of 1000 random trials is performed to account for the random nature of road roughness. Assuming a typical population standard deviation of 2 to 3 micro-strain, a 95% confidence interval yields an estimated margin of error of approximately 0.1–0.2 micro-strain. The best fit distribution and the maximum likelihood estimate parameters for the filtered dynamic response are then found using the Kolmogorov–Smirnov (KS) test in MATLAB. The adequacy of filtering is then measured using the value of the probability for the filtered signal to contain the static response. A bound of ± 1 micro-strain is considered as a tolerance value for the static response, since it is the least resolution one can achieve in the field for electrical strain gauges.

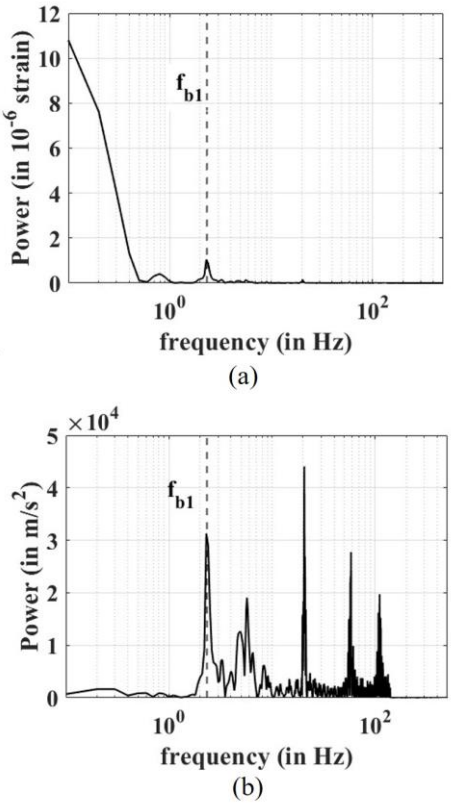

Figure 1. FFT plots of (a) bridge dynamic strain response (b) acceleration response.

3 IMPLEMENTATION DETAILS

3.1 Vehicle Bridge Interaction Modeling

The vehicle is modeled using a half-car model (HCM) as shown in Figure 2. The bridge is modeled as a simply supported Euler-Bernoulli beam. In HCM, four degrees of freedom are considered – vertical displacement (z_v) and pitching rotation

DOI: 10.3217/978-3-99161-057-1-160

(θ_v) of the vehicle's center of gravity (CG), vertical displacement of the front (z_{tf}) and rear tires (z_{tr}). The vehicle's sprung mass is represented by M_v, pitching moment of inertia as I_v, front and rear suspension stiffness k_{sf} and k_{sr} and front and rear suspension damping as c_{sf} and c_{sr} respectively. The axle spacing between the two axles is 's' and the distances of CG from the front axle and the rear axle are denoted by s_1 and s_2. The displacements of the bridge at the contact points corresponding to the front and rear tires are u_{cf} and u_{cr} respectively. The road roughness profile at the contact points is represented by r_{cf} and r_{cr}. The equation of motion for the vehicle's bouncing motion can be given by taking vertical force equilibrium as,

$$M_v\ddot{z}_v + c_{sf}\left(\dot{z}_v + \dot{\theta}_v s_1 - \dot{z}_{tf}\right) + k_{sf}\left(z_v + \theta_v s_1 - z_{tf}\right) + c_{sr}\left(\dot{z}_v - \dot{\theta}_v s_2 - \dot{z}_{tr}\right) + k_{sr}(z_v - \theta_v s_2 - z_{tr}) = 0 \quad (1)$$

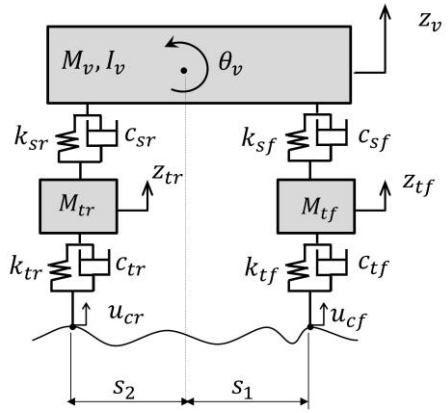

Figure 2. Half car model.

The equation of motion for the vehicle's pitching motion can be found by taking moment equilibrium about the vehicle's CG axis as:

$$I_v\ddot{\theta}_v + c_{sf}\left(\dot{z}_v + \dot{\theta}_v s_1 - \dot{z}_{tf}\right)s_1 + k_{sf}\left(z_v + \theta_v s_1 - z_{tf}\right)s_1 - c_{sr}\left(\dot{z}_v - \dot{\theta}_v s_2 - \dot{z}_{tr}\right)s_2 - k_{sr}(z_v - \theta_v s_2 - z_{tr})s_2 = 0 \quad (2)$$

The equation of motion for the vertical displacements of the front and rear tires can be found as:

$$m_{tf}\ddot{z}_{tf} - c_{sf}\left(\dot{z}_v + \dot{\theta}_v s_1 - \dot{z}_{tf}\right) - k_{sf}\left(z_v + \theta_v s_1 - z_{tf}\right) + c_{tf}\left(\dot{z}_{tf} - \dot{u}_{cf} - v r'_{cf}\right) + k_{tf}\left(z_{tf} - u_{cf} - r_{cf}\right) = 0 \quad (3)$$

$$m_{tr}\ddot{z}_{tr} - c_{sr}\left(\dot{z}_v - \dot{\theta}_v s_2 - \dot{z}_{tr}\right) - k_{sr}(z_v - \theta_v s_2 - z_{tr}) + c_{tr}\left(\dot{z}_{tr} - \dot{u}_{cr} - v r'_{cr}\right) + k_{tr}(z_{tr} - u_{cr} - r_{cr}) = 0 \quad (4)$$

Finally, the bridge's flexural vibration equation is given by,

$$EI\, u^{iv}(x,t) + m\,\ddot{u}(x,t) + c\,\dot{u}(x,t) = \left[-\frac{M_v g}{2} - m_{tf}g + c_{tf}\left(\dot{z}_{tf} - \dot{u}_{cf} - v r'_{cf}\right) + k_{tf}\left(z_{tf} - u_{cf} - r_{cf}\right)\right]\delta(x - vt) + \left[-\frac{M_v g}{2} - m_{tr}g + c_{tr}\left(\dot{z}_{tr} - \dot{u}_{cr} - v r'_{cr}\right) + k_{tr}(z_{tr} - u_{cr} - r_{cr})\right]\delta(x - (vt - s)) \quad (5)$$

Using the modal superposition technique, the displacement $u(x,t)$ can be represented using,

$$u(x,t) = \sum_{n=1}^{N} q_n(t)\varphi_n(x) \quad (6)$$

where $q_n(t)$ is the modal coordinate and $\varphi_n(x)$ represents the nth mode shape of the simply supported beam, and N represents the total number of modes used. Now, substituting Equation (6) in Equations (1), (2), (3), (4), and (5), and then using the modal orthogonality principle, the vehicle bridge interaction system can be represented in a matrix form as follows:

$$[M]\{\ddot{X}\} + [C]\{\dot{X}\} + [K]\{X\} = \{R\} \quad (7)$$

where $[M], [C]$ and $[K\}$ represent the mass, damping, and stiffness matrix of the VBI system of size $(N+4)\times(N+4)$. $\{R\}$ represents the force vector and $\{\ddot{X}\}$, $\{\dot{X}\}$ and $\{X\}$ represents the acceleration, velocity, and displacement vector, respectively, of size $(N+4)\times 1$. This equation is coded in MATLAB and solved using Newmark's technique (constant acceleration). In this study, road roughness is modeled as a random process with a normal distribution. The wavelength characteristics are characterized using the spectral density of the profile height. The power spectral density coefficients from [10] are adopted to represent various classes of road roughness. A typical roughness profile is shown in Figure 3.

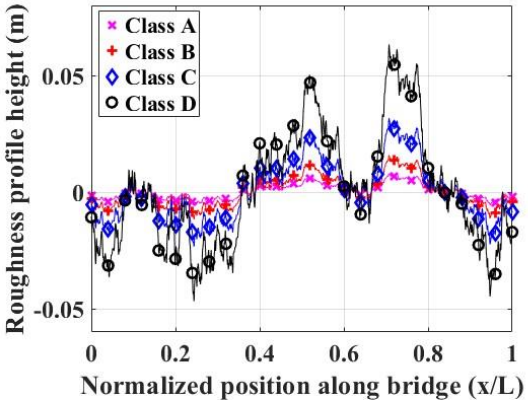

Figure 3. A typical roughness profile.

3.2 *Validation of the HCM code*

The code for vehicle bridge interaction is validated using data from the literature [9]. The values of the VBI parameters taken are as follows.

Vehicle: M_v = 1794.4 kg; m_{tf} = 87.15 kg; m_{tr} = 140.4 kg; s_1 = 1.271m; s_2 = 1.713 m; I_v =3443.03 kgm^2; k_{sf} =66.824 kN/m; k_{sr} =18.615 kN/m; $k_{tf} = k_{tr}$ = 101.12 kN/m; $c_{tf} = c_{tr}$ = 0 Ns/m; c_{sf} = 1190 Ns/m; c_{sr} = 1000 Ns/m; v = 40 km/h; Bridge: m =20000 kg/m; L =100 m; E = 207 GPa; I = 0.174 m^4; Roughness: Smooth. The mid-span displacement of the bridge obtained using the developed code matched well with that from the literature, as shown in Figure 4.

3.3 *Numerical data taken in the study*

The half-car vehicle model values are taken from the representative vehicle data set from TruckMaker software. For the bridge, the values of a typical 50m span prestressed box

DOI: 10.3217/978-3-99161-057-1-160

girder for three lane traffic are considered. And, for road roughness, the parameter values were taken from [10], [11] and [12]. The numerical values are given below.

Vehicle: M_v =22700 kg; $m_{tf} = m_{tr}$ =1500 kg; I_v =71,761.1 kg/m^2; $s_1 = 3.133$ m; s_2 =1.667 m; k_{sf} =25000 N/m; k_{sr} =30000 N/m; $k_{tf} = k_{tr} = 1.273 \times 10^6\ N/m$; $c_{tf} = c_{tr} = 6000\ Ns/m$. Bridge: $m = 11880\ kg/m$; $L = 50\ m$; $A = 4.87\ m^2$; $I = 4.923\ m^4$; $E = 31.62\ GPa$; $\nu = 0.2$; $f_{b1} = 2.31\ Hz$

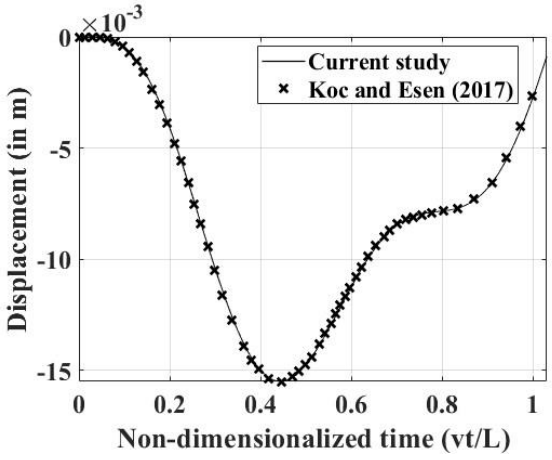

Figure 4. Validation of HCM code.

3.4 Modal Convergence study

As the method uses modal superposition, the minimum number of modes required to accurately represent the results are found using a convergence study. Towards this, absolute (δ_{abs}) and relative (δ_{rel}) convergence is checked wherein the definition used is,

$$\delta_{abs} = \| \in_{N=N_{max}} - \in_{N=1} \| \tag{8}$$

$$\delta_{rel} = \| \frac{\in_{N=N_{max}} - \in_{N=1}}{\in_{N=N_{max}}} \| \times 100\% \tag{9}$$

where N represents the number of modes used; N_{max} represents the maximum number of modes used; ϵ represents the maximum strain value at the given number of modes. The tolerance limit was kept at 0.01 micro-strain for absolute convergence and 0.01% for relative convergence. The convergence study was performed for various vehicle speeds ranging from 20 km/h to 120 km/h and for four roughness classes as per [10]. The minimum number of modes required to achieve convergence of the maximum axial strain response is shown in Table 1 and Table 2 respectively. It was found that 53 modes were adequate to satisfy the tolerance. Hence, further in the study, 60 modes were considered for all the computations.

Table 1. Modal convergence study based on absolute convergence for maximum axial strain at L/2.

Roughness Class	Speed (in km/h)					
	20	40	60	80	100	120
Class A	31	27	17	23	11	27
Class B	29	19	11	23	13	27
Class C	27	11	11	21	11	29
Class D	27	11	13	11	29	15

4 RESULTS

4.1 Filtered and Unfiltered response

To demonstrate the filtering process, as a reasonable estimate, a cutoff frequency of half the bridge's natural frequency is taken. The dynamic response of the bridge is simulated for 1000 random trials of road roughness. Assuming the velocity to be 50 km/h and road roughness as class D, the maximum midspan axial strain and average shear strain sum of the unfiltered and filtered signals are shown in Figure 5 and Figure 6 respectively.

Table 2. Modal convergence study based on relative convergence for maximum axial strain at L/2.

Roughness Class	Speed (in km/h)					
	20	40	60	80	100	120
Class A	31	29	17	31	15	29
Class B	31	31	17	31	31	31
Class C	29	19	13	31	29	31
Class D	29	11	31	17	29	15

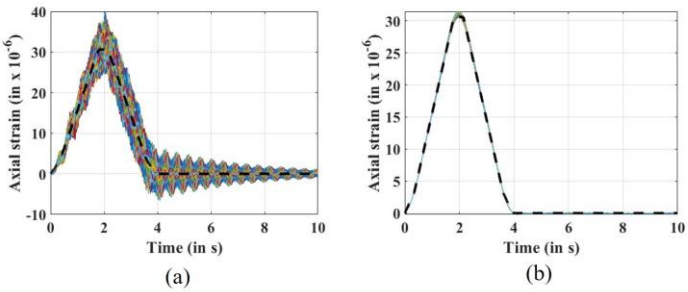

Figure 5. Monte Carlo simulation of (a) unfiltered and (b) filtered dynamic response of 1000 random trials for maximum axial strain at L/2 (dashed line represents the static response).

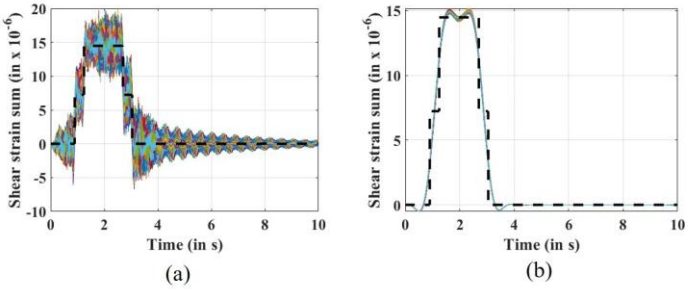

Figure 6. Monte Carlo simulation of (a) unfiltered and (b) filtered dynamic response of 1000 random trials for average shear strain sum at L/4 and 3L/4 (dashed line represents the static response).

The histogram plot for the maximum axial strain and average shear strain sum for 1000 trials is shown in Figure 7(a) and Figure 7(b) respectively. One can observe that filtering makes the unfiltered response come closer to the static response. This observation was not much in the case of the average shear strain sum. Various probability distributions that can sufficiently fit the filtered histogram data were checked using the maximum log likelihood values in MATLAB. The plot of various distributions fitting the histogram data is shown in Figure 8.

DOI: 10.3217/978-3-99161-057-1-160

A Kolmogorov-Smirnov (KS) test is used to check whether two samples come from the same distribution or not. Here, one sample is from the Monte-Carlo simulation data, and the other sample is from the fitting distribution (Normal, Lognormal, Logistic, Weibull, Gamma, etc.). The null hypothesis is that both come from the same distribution, and the alternative hypothesis is that both come from different distributions. A p-value of 0.05 is used to denote the significance level for the null hypothesis to be true. The distribution that gives the highest p-value and the log likelihood value is chosen as the best fit distribution, and its probability density value at the static response is calculated.

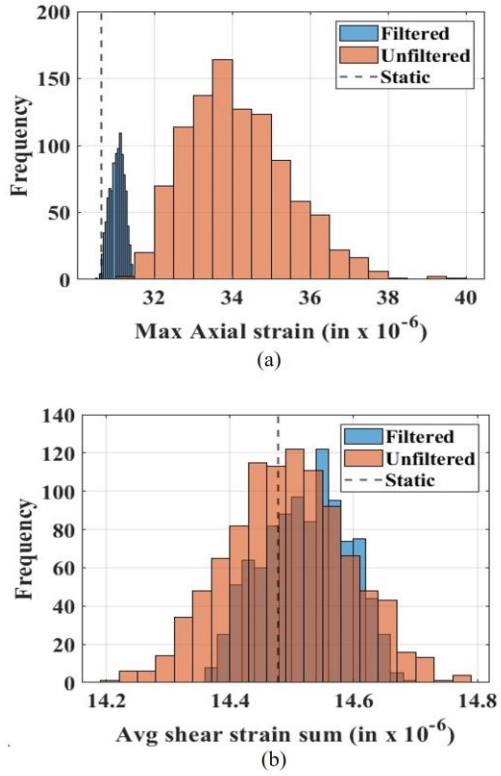

Figure 7. Histogram plot for the (a) Maximum axial strain (b) Average shear strain sum data.

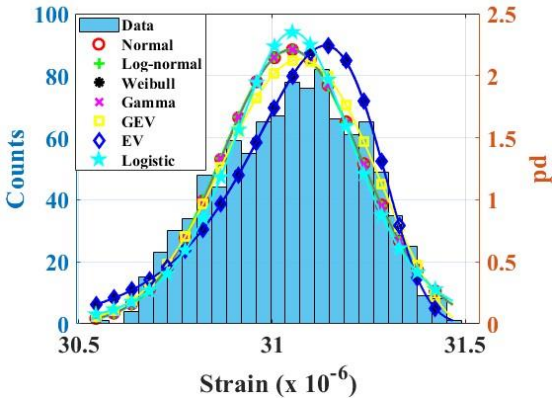

Figure 8. Best fit probability distribution for strain data.

The maximum likelihood estimates (MLE) parameters, KS2 test results, and their corresponding p-value for various distributions are shown in Table 3 and Table 4. One can observe that for the unfiltered response, the Generalized Extreme Value (GEV) distribution has passed the test with the highest p-value of 0.9104. For the case of filtered response, all the distributions tested gave the pass results, but again, GEV has the highest p-value of 0.7167. Hence, the probability that the GEV distribution contains the static response ± 1 micro-strain for the filtered and unfiltered response will be 1.0000 and 0.0086, respectively.

4.2 Study of static response probability for different cutoff frequency coefficients

The cutoff frequency was taken as a multiple of the bridge's natural frequency. This multiple will be referred to as the cutoff frequency coefficient. The range of coefficients from 0.2 to 1.5 was studied. The variation of the probability value of the static response for this range of coefficients is shown in Figure 9(a) and Figure 9(b) for a given vehicle speed of 50 km/h and road roughness class D. For the case of axial strain in Figure 9(a), it is observed that the probability value becomes zero at very low cutoff frequency (here for 0.1 and 0.15). This implies that there are not enough frequency components in the filtered response to represent the static value. Hence, the distribution of the filtered response will lie much farther away from the static response. A typical histogram plot for this case is shown in Figure 10(a) and Figure 10(b) for a cutoff frequency of $0.15f_{b1}$. One can observe that the filtered values are much lower than the static value. For all the values after 0.1, the probability becomes greater than 0. This means that the probability of static response lying in ±1 micro-strain bound of the filtered response is greater than that of the unfiltered response. This demonstrates the effect of filtering. The maximum effect is observed at the one with the highest probability value. i.e., in this case, for a cutoff frequency of 0.45 f_{b1}. For the case of shear strain sum shown in Figure 9(b), the static response probability becomes almost close to 1.0 for all the cutoff coefficients above 0.1. This is because, for shear strain sum, the average value was taken. Even for the case without filtering, one can achieve a response value closer to the static value, as evident from Figure 7(b). Hence, filtering doesn't have much of an effect in this case.

Table 3. Maximum Likelihood Estimates, KS Test results, and probability values to contain the static response for various distributions of unfiltered responses.

Distribution	*MLE parameter*	*KS test*	*p-value*	*Probability*
Normal	μ=34.13 σ = 1.311	Pass	0.1768	0.0282
Log-normal	μ=3.527 σ = 0.038	Pass	0.3078	0.0240
Weibull	a=34.79 b = 23.82	Fail	9.8e-6	0.0773
Gamma	α=686.3 β =0.049	Pass	0.2580	0.0253
GEV	μ=-0.1005 σ = 1.146 ξ = 33.57	Pass	0.9104	0.0086
EV	μ=34.82 σ = 1.494	Fail	4.6e-7	0.0815
Logistic	μ=34.07 β = 0.750	Pass	0.3078	0.0351

DOI: 10.3217/978-3-99161-057-1-160

Table 4. Maximum Likelihood Estimates, KS Test results, and probability values to contain the static response for various distributions of filtered response.

Distribution	*MLE parameter*	*KS test*	*p-value*	*Probability*
Normal	μ=31.05 σ = 0.18	Pass	0.5295	0.9994
Log-normal	μ=3.435 σ = 0.006	Pass	0.4938	0.9994
Weibull	a=31.14 b = 189.7	Pass	0.2355	0.9999
Gamma	α=29566 β =0.0011	Pass	0.5295	0.9994
GEV	μ=-0.368 σ = 0.187 ξ = 30.99	Pass	0.7167	1.0000
EV	μ=31.14 σ =0.164	Pass	0.2145	0.9999
Logistic	μ=31.03 β = 0.106	Pass	0.2355	0.9959

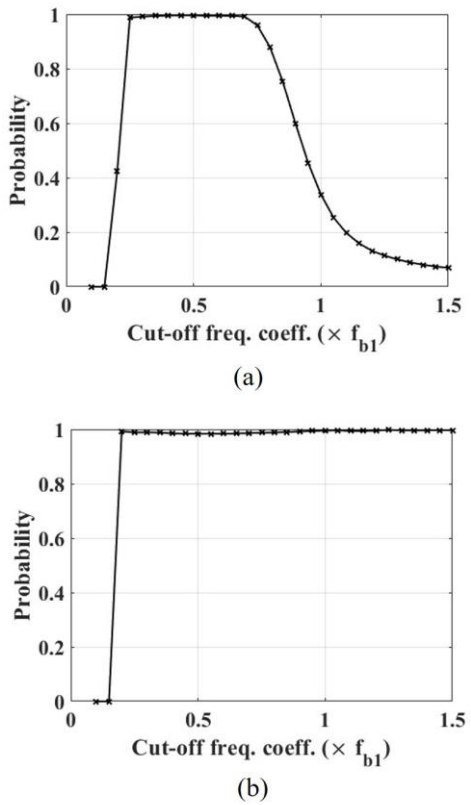

Figure 9. Variation of cutoff frequency coefficients with the static response probability of the filtered signal – (a) Maximum axial strain at L./2 (b) Average shear strain sum at L/4 and 3L/4.

4.3 Effect of vehicle speed

The effect of vehicle speed is studied by taking speed values as 10 km/h, 25 km/h, 50 km/h, and 100 km/h. The road roughness and bridge natural frequency were kept constant at class D and 2.31 Hz. The static response probability values for different cutoff frequencies are shown in Figure 11 for maximum mid-span axial strain and in Figure 12 for the average shear strain sum. We can observe that the minimum cutoff required to attain a probability value of 1.0 increases with increasing speed. For instance, the minimum cutoff coefficients for speed values of 10, 25, 50, and 100 km/h are $0.1f_{b1}$, $0.15f_{b1}$, $0.25f_{b1,}$ and $0.4f_{b1,}$ respectively. This is because of the shifting of the driving frequency with the increase in speed. Also, the region from 0.45 f_{b1} to 0.75 f_{b1} has the probability value of 1.0 in all the cases and is hence recommended.

For shear strain sum, the effect of speed is observed in Figure 12. Again, the effect of driving frequency on the minimum cutoff coefficient can be observed. Also, after the minimum cutoff, at all the cutoff coefficients, the static response probability is maintained at 1.0, which was not observed in the axial strain case. This is because of the same advantage of taking the average value in the case of shear strain sum, as explained previously.

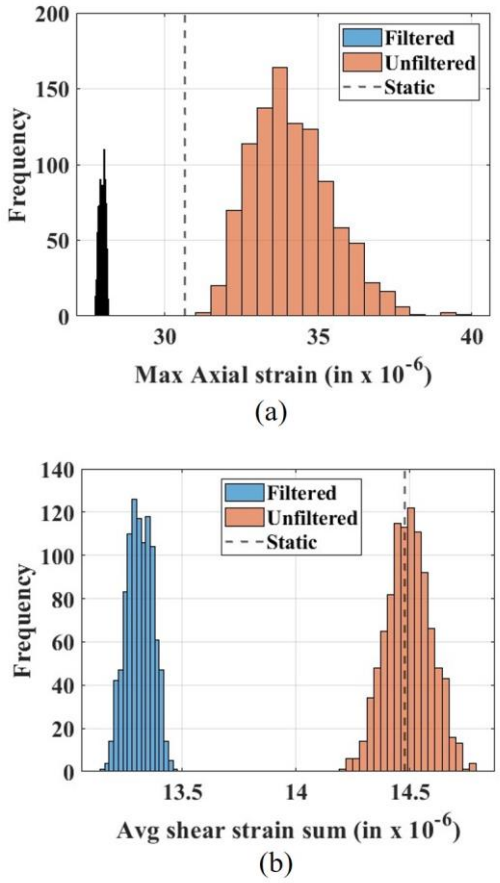

Figure 10. Histogram plot for filtered and unfiltered response corresponding to cutoff frequency of $0.15f_{b1}$ for (a) Maximum axial strain at L/2 (b) Average shear strain sum at L/4 and 3L/4.

DOI: 10.3217/978-3-99161-057-1-160

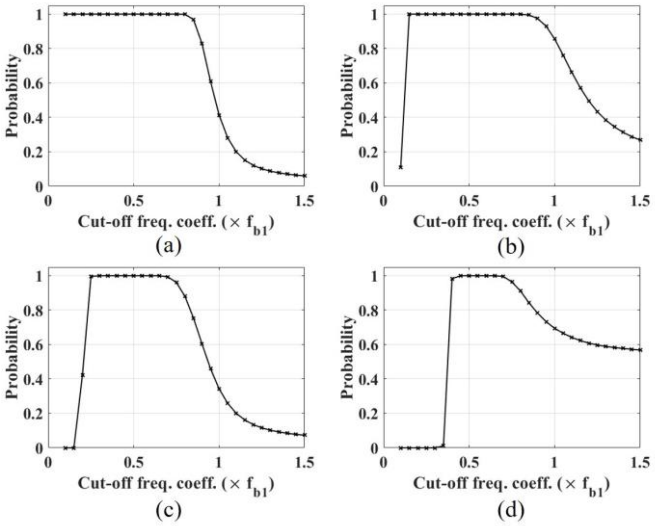

Figure 11. Effect of vehicle speed (a) v=10 km/h (b) v = 25 km/h (c) v = 50 km/h (d) v = 100 km/h – Maximum axial strain at L/2 for f_{b1} = 2.31 Hz and roughness class D.

4.4 Effect of road roughness

The effect of road roughness is studied by varying the road roughness from class A (Very Good) to class D (Poor). The vehicle velocity is kept constant at 50 km/h, and the natural frequency is at 2.31 Hz. The static response probability values for different cutoff frequencies are shown in Figure 13 and Figure 14 for maximum mid-span axial strain and average shear strain sum, respectively. It can be observed that for low roughness classes, the probability is 1.0 even at higher cutoff frequencies. As the roughness class increases, the static response probability decreases. This is because a higher degree of roughness corresponds to increased dynamic noise in the signal and hence a decrease in the static response probability value. For the case of the average shear strain sum in Figure 14, there was not much observation. The probability value reaches 1.0 for all the cutoff coefficients above 0.15.

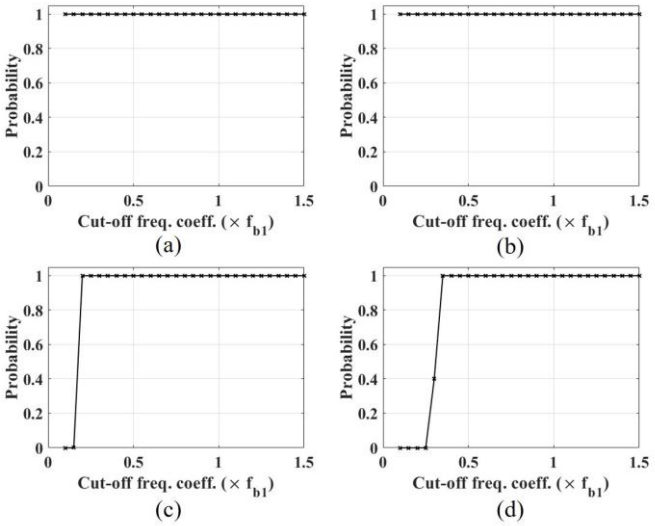

Figure 12. Effect of vehicle speed (a) v=10 km/h (b) v = 25 km/h (c) v = 50 km/h (d) v = 100 km/h – Average shear strain sum at L/4 and 3L/4 for f_{b1} = 2.31 Hz and roughness class D.

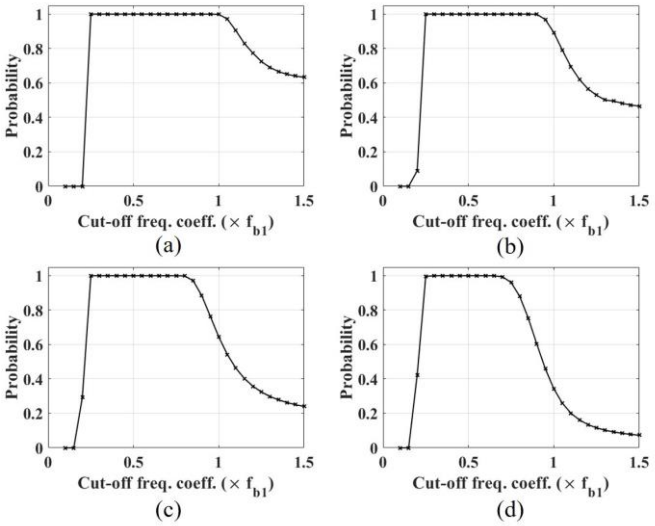

Figure 13. Effect of road roughness (a) Class A (b) Class B (c) Class C (d) Class D – Maximum axial strain at L/2 for f_{b1} = 2.31 Hz and v=50 km/h.

4.5 Effect of bridge natural frequency

Finally, the effect of various bridge natural frequencies is studied. The natural frequency of the bridge is varied by changing the value of the flexural rigidity of the bridge. Four values of natural frequency – 2.31 Hz, 5 Hz, 7.5 Hz, and 10 Hz were studied, corresponding to four EI values – 157 GNm^2, 753 GNm^2, 1693 GNm^2, and 3008 GNm^2.

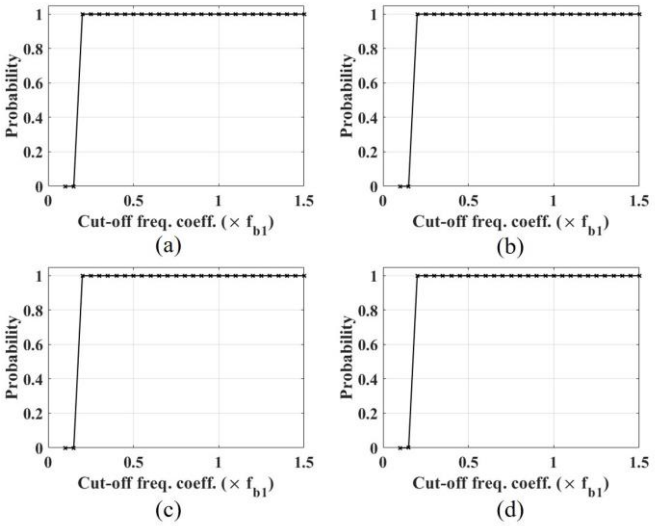

Figure 14. Effect of road roughness (a) Class A (b) Class B (c) Class C (d) Class D –Average shear strain sum at L/4 and 3L/4 for f_{b1} = 2.31 Hz and v=50 km/h.

DOI: 10.3217/978-3-99161-057-1-160

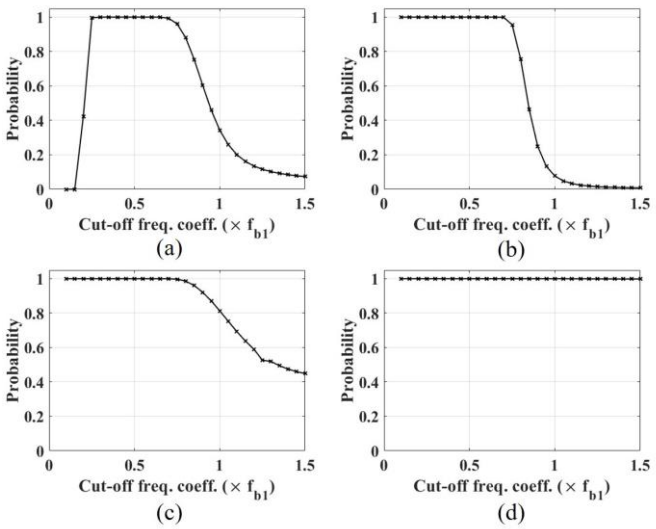

Figure 15. Effect of bridge natural frequency (a) f_{b1} = 2.31 Hz (b) f_{b1} = 5 Hz (c) f_{b1} = 7.5 Hz (d) f_{b1} = 10 Hz – Maximum axial strain at L/2 for v =50 km/h and roughness class D.

For all the coefficients between 0.25 f_{b1} to 0.7 f_{b1}, the static response probability for the case of maximum axial strain is 1.0, irrespective of different natural frequencies, as shown in Figure 15. Also, it can be observed that for a given case of a cutoff frequency closer to the bridge's natural frequency, the static response probability depends upon the relative distance between the driving frequency and the bridge's natural frequency. If this difference is high, the probability value becomes 1.0; otherwise, the value reduces. The figure for the average shear strain sum is shown in Figure 16. As observed previously, the probability value for most of the cutoff coefficients is 1.0.

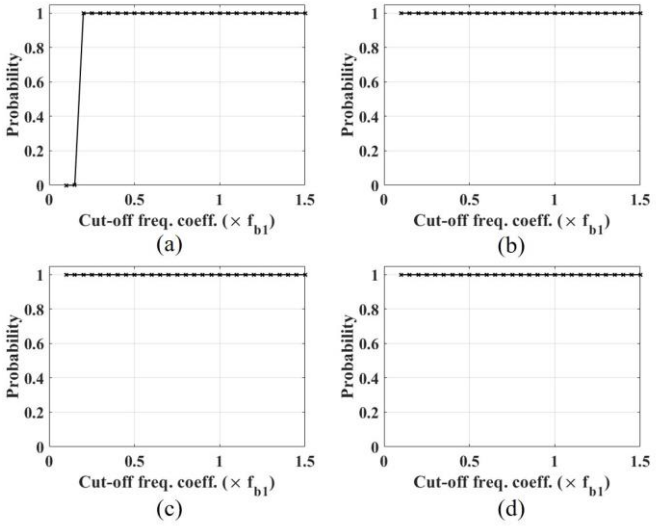

Figure 16. Effect of bridge natural frequency (a) f_{b1} = 2.31 Hz (b) f_{b1} = 5 Hz (c) f_{b1} = 7.5 Hz (d) f_{b1} = 10 Hz – Average shear strain sum at L/4 and 3L/4 for v = 50 km/h and roughness class D.

5 CONCLUSION

The idea of cutting off the higher frequencies from the bridge strain response to get the static response of the bridge is investigated. A half-car vehicle bridge interaction model was used to simulate the motion of a moving vehicle. Newmark's constant integration scheme was used to solve the program in MATLAB.

A Monte Carlo simulation of 1000 trials is performed for random values of road roughness. A low-pass Butterworth filter is used to cut off higher frequencies. Contrary to the literature studies wherein the cutoff frequency was related to the driving frequency, in this study, it is related to the bridge's natural frequency. A detailed study on the influence of the cutoff frequency so that the filtered signal contains the static response ±1 micro-strain is undertaken. And finally, the effect of VBI parameters – vehicle speed, road roughness, and natural frequency was studied. From the study, the following is inferred:

i. The cutoff frequency of 0.5 times the bridge natural frequency seems to have the highest probability of containing the static strain response across different vehicle speeds, road roughness, and natural frequency of the bridge.
ii. The higher the vehicle speed, the higher is the driving frequency, and hence the cutoff frequency to contain the static response increases.
iii. The higher the road roughness, the higher the dynamic noise in the response, and hence, the static response probability decreases for a given cutoff frequency.
iv. Both the driving frequency and the bridge natural frequency determine the cutoff frequency, which would contain the static strain response.

Further efforts are required to validate the study using field data.

ACKNOWLEDGMENT

Sarath R. gratefully acknowledges the Ministry of Education, Government of India, for supporting this work through the Prime Minister's Research Fellowship scheme.

REFERENCES

[1] P. Pitchai, U. Saravanan, and R. Goswami, Mechanics-based algorithms to determine the current state of a bridge using quasi-static loading and strain measurement. Structural Health Monitoring, 18 (5-6), 1874-1888, 2018.
[2] T. M. Deepthi, U. Saravanan, and A. Meher Prasad, Algorithms to determine wheel loads and speed of trains using strains measured on bridge girders. Structural Control and Health Monitoring, 26(1), e2282, 2019.
[3] M. I. S. Elhelbawey, Definition of improved modeling procedures for the analysis of bridge structures under truck loading using Weigh in Motion. PhD Thesis, University of Maryland, College Park, USA, 1991.
[4] G. Thater, P. Chang, D. Schelling, and C. Fu, Estimation of bridge static response and vehicle weights by frequency response analysis. Canadian Journal of Civil Engineering, 25(4), 631-689, 1998.
[5] T. H. Chan and T. Yung, A theoretical study of force identification using prestressed concrete bridges, Engineering Structures, 22(11), 1529-1537, 2000.
[6] C. Mustafa, I. Yoshida, and H. Sekiya, An investigation of bridge influence line identification using time-domain and frequency domain methods. In Structures, 33, 2061-2065, Elsevier, 2021.
[7] H. Wang, Q. Zhu, J. Li, J. Mao, S. Hu, and X. Zhao, Identification of moving train loads on railway bridges based on strain monitoring, Smart Structures System, 23(3), 263-278, 2019.
[8] A. Aloisio and R. Alaggio, Experimental estimation of elastic modulus of concrete girders from drive-by inspections with force balance accelerometers. Shock and Vibrations, 2021(1), 1617526, 2021.
[9] M. A. Koc and I. Esen, Modelling and analysis of vehicle-structure road coupled interaction considering structural flexibility, vehicle parameters,

DOI: 10.3217/978-3-99161-057-1-160

and road roughness. Journal of Mechanical Science and Technology, 31, 2057-2074, 2017.
[10] ISO 8608, Mechanical vibration road surface profiles – reporting of measured data, 2016.
[11] J. Oliva, J. M. Goicolea, P. Antolin, and M. A. Astiz, Relevance of a complete road roughness description in vehicle bridge interaction dynamics, Engineering Structures, 56, 466-476, 2013.
[12] Y. Zhan and F. Au, Bridge surface roughness identification based on vehicle bridge interaction. International Journal of Structural Stability and Dynamics, 19(07), 1950069, 2019.